EasyChair Preprint

№ 6676

Image Prior Transfer and Ensemble Architectures for Parkinson's Disease Detection

Tahjid Ashfaque Mostafa and Irene Cheng

September 23, 2021

Image Prior Transfer and Ensemble Architectures for Parkinson's Disease Detection*

Tahjid Ashfaque Mostafa[1 [0000−0003−3033−635X]] and Irene Cheng[1 [0000−0001−9699−4895]]

Department of Computing Science, University of Alberta, Edmonton, AB T6G 2E8, Canada
{tahjid,locheng}@ualberta.ca

Abstract. Neural networks have shown promising results in many applications including computer aided diagnosis systems. However, insufficient effort has been expended on model knowledge transfer combined with ensemble architecture structures. Here, our use case focuses on detecting Parkinson's Disease (PD) by automatic pattern recognition in brain magnetic resonance (MR) images. In order to train a robust neural network, sufficiently large amount of labeled MR image data is essential. However, this is challenging because ground truth data needs to be labeled by clinical experts, who often have busy daily schedules. Furthermore, brain MR images are not often captured for PD patients. Therefore, we explore the effectiveness of pre-training neural networks using natural images instead of brain MR images of PD patients. We also propose different ensemble architecture structures, and demonstrate that they outperform existing models on PD detection. Experimental results show that our detection performance is significantly better compared to models without prior training using natural images. This finding suggests a promising direction when no or insufficient MR image training data is available. Furthermore, we performed occlusion analysis to identify the brain regions that the models focused on to deliver higher performance on PD detection during the decision making process.

Keywords: Parkinson's Disease Detection · Model Knowledge Transfer · Ensemble Learning · Deep Learning · Magnetic Resonance Imaging.

1 Introduction

Computer aided diagnosis systems based on brain imaging have shown merits in the diagnosis of Parkinson's Disease (PD) by automatic recognition of patterns that characterize symptoms. PD is the second most common neurodegenerative disorder and the most common movement disorder affecting the elderly next to the Alzheimer's disease [23]. PD is caused by the loss of neurons in the Substantia Nigra region of the brain, responsible for the production of Dopamine.

* Supported by Multimedia Research Center (MRC), Department of Computing Science, University of Alberta, Edmonton, Canada.

It facilitates the communication between neurons for body movement coordination, and a shortage of dopamine will lead to PD. PD has been associated with neurological symptoms like speech impediments, olfactory dysfunctions, sleep disorders, autonomic dysfunctions, fatigue and motor symptoms like tremors, Bradykinesia, postural instability, rigidity of the limbs, impaired gait etc. It has been clinically studied for a long time, but the exact causes leading to PD are still not properly identified [24]. PD is usually diagnosed with motor symptoms, which might not become apparent until 50%-70% of the neurons have been damaged [25], when it is too late for any effective preventive measures. A guaranteed cure for PD has not been discovered, but early detection might offer an opportunity for slowing or stopping the progression of the disease. New forms of treatment like Exenatide [26], show promising results with cases where PD was detected in the initial stages. One of the techniques that has been found to be successful in detecting neurodegenerative diseases with cognitive impairments is the analysis of the structural changes in the brain using Medical Imaging techniques, such as MR images, which provide high contrast and resolution within soft tissue. Inspired by the promising performance of machine learning in recent years, researchers attempted to apply neural networks in analyzing brain MR images to diagnose neurodegenerative diseases, including PD. The challenge lies in the lack of a sufficiently large amount of labeled data, which is critical in order to train a robust neural network. Note that MR images are seldom taken from PD patients, and even if they are available, they are not properly labeled. In this work, (1) we explore the feasibility of detecting PD by first pre-training neural networks using a large quantity of more widely available natural images, before training with a limited set of brain MR images of PD patients, (2) we propose different ensemble architecture structures and analyze which structures can deliver higher PD detection accuracy, (3) we compare the performances between models with and without being pre-trained on natural images and (4) we identify the key regions of the brain in the decision making process using occlusion analysis. In this context, the natural images are taken from the Imagenet [7] dataset. Experimental results show that we achieve over 90% detection accuracy for all our proposed architectures with the highest being 96.3%, which is significantly better than existing models. We also found that using models pre-trained on the Imagenet [7] dataset yields much better performance than just training the model with the limited set of PD MR images.

2 Background and Related Works

Many Machine Learning (ML) and Deep Learning (DL) based approaches have been introduced for the detection of Parkinson's Disease (PD). Babu et al. [2] achieved a 87.21% accuracy in classifying PD using Gray Matter (GM) with a Computer Aided Diagnosis (CAD) system. Rana et al. [3] used a Support Vector Machine (SVM) for classification with t-test feature selection on White Matter (WM) and GM, and also on Cerebrospinal Fluid (CSF). They achieved 86.67% accuracy for GM and WM, and 83.33% accuracy for CSF. In another work [4],

Table 1: Demographic Data

	PD	HC	Average
Age(Years)	62.0 ± 9.54	49.2 ± 16.9	55.6 ± 15.1
Sex (Male / Female)	189 / 110	172 / 127	361 / 237

the authors used the relation between tissues instead of considering the tissues separately and achieved an accuracy of 89.67%. Radial Basis Function Neural Network (RBFNN) was used by Pazhanirajan et al. [27] for PD classification. Tahjid et al [22], demonstrated that an ensemble architecture trained on only WM and GM data performed better than using the whole brain MR scan for detecting PD. In this work, we explore the feasibility of supplementing the training set with natural images (non-PD related) before using a limited set of PD MR images. We also explore 3 ensemble architectures with two model blocks to process WM and GM separately. The proposed architectures were first pre-trained using non-PD related ImageNet [7] (natural) images. We then further trained the architectures with MR images. We separated WM and GM from the MR scans of the brain, and passed them through our architectures separately.

3 Proposed Method

3.1 Dataset

For MR images, We used Parkinson Progression Markers Initiative (PPMI) dataset [5], which consists of T1-weighted sMRI scans for 568 PD and Healthy Control (HC) subjects. We only chose 445 subjects and discarded the rest due to structural anomalies during preprocessing steps. There was a class imbalance in the resulting data with 299 PD and 146 HC subjects. To balance the data, we collected 153 HC T1-weighted sMRI scans from the publicly available IXI dataset [6]. The final dataset was class balanced with 598 subjects. The demographic for the dataset is presented in Table 1. Note that the total of 598 subjects is still regarded as insufficient for learning-based model training. Thus, our strategy is to start from models pre-trained with natural images. The dataset was generated following the works of West et al [28].

3.2 Preprocessing

The preprocessing pipeline from Tahjid et al. [22] was used for preprocessing the data, which gave us WM (with and without smoothing) and GM (with and without smoothing); 4 categories in total.

3.3 Models

We selected six existing models of the ImageNet Large Scale Visual Recognition Challenge (ILSVRC) [8] implemented in Pytorch [10], to form various model block combinations.

– ResNet 101 [16], SqueezeNet 1.1 [17], DenseNet 201 [18], VGG 19 [19], MobileNet V2 [20], ShuffleNet V2 [21]

The six ILSVRC models are available from Torchvision [11] in two versions: without any training (untrained) and trained on the ImageNet dataset. We trained and tested each model on the MRI data. We then chose the top performing model combinations to create ensemble architectures. The same model block design was used to process the WM, and GM input. We used both untrained and pre-trained models to construct our ensemble model blocks and compared the performances of the resultant architectures to examine if training on the non-PD related ImageNet dataset makes the architectures perform better in PD detection. Since the six models were originally designed to process the ImageNet dataset, we had to modify the input layers of all models to accommodate the format of our MRI input and the output layers were changed to predict between 2 classes (PD and HC) instead of the 1000 ImageNet classes. Based on the top performing model combinations, we propose different architectures described below.

3.4 Ensemble Architecture 1

For this architecture, all six models were stacked as shown in Figure 1. This design was created with only one data modality in mind. Two versions (untrained and pre-trained) of this model was trained with GM and WM scans separately. The output from all six models was passed through a ReLU layer followed by a linear layer to predict the output.

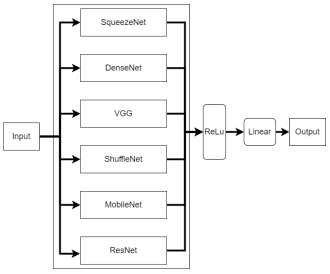

Fig. 1: Ensemble Architecture 1

3.5 Ensemble Architecture 2

The extracted GM and WM scan dimension was $121 \times 145 \times 121$. We passed them in parallel through two model blocks, each of which was comprised of multiple ILSVRC models. We then concatenated the output from both blocks and passed them through a ReLU activation layer followed by a final linear layer, which predicted between the two output classes (PD and HC). Fig. 2 shows a visual representation of this architecture. We used 3 different model block designs.

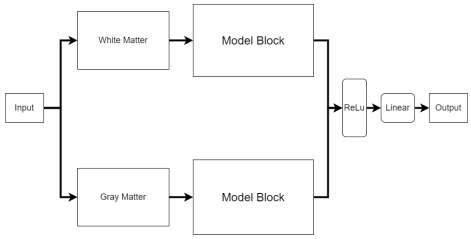

Fig. 2: Ensemble Architecture 2

Design 1 - TriNet1 The model block was comprised of DenseNet, ShuffleNet and SqueezeNet in parallel. The input was passed through all three models simultaneously, as shown in Fig. 3a.

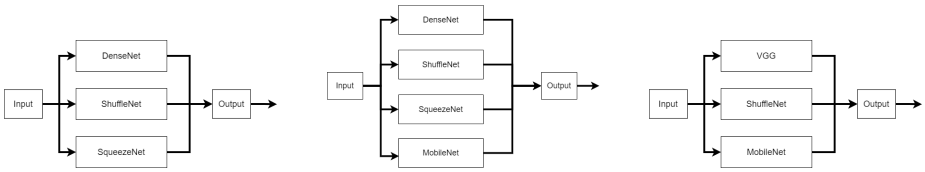

(a) Design 1 : TriNet1 (b) Design 2 : QuadNet (c) Design 3 : TriNet2

Design 2 - QuadNet The model block was created by adding MobileNet to Model Block 1, so it was comprised of DenseNet, ShuffleNet, SqueezeNet and MobileNet in parallel. The input was passed through all four models simultaneously, as shown in Fig. 3b.

Design 3 - TriNet2 The model block was created with ShuffleNet, VGG and MobileNet in parallel. The input was passed through all three models simultaneously, as shown in Fig. 3c

4 Experimental Results

We had two separate versions for each of our ensemble architectures: constituent models untrained and pre-trained with ImageNet data. The brain MR dataset was randomly split and 80% was selected for training and 20% for testing. At each epoch, the training set was further split randomly and 20% was selected for validation. The models were trained with various learning rates including **0.01**, **.001** and **.0001** and the process was repeated 5 times. For reference purpose, Table 2 presents the results of some existing approaches using similar data.

Table 2: Accuracy results of some related works analyzing WM and GM

Source	Accuracy
Focke et al.[1] [GM]	0.3953
Focke et al.[1] [WM]	0.4186
Babu et al.[2] [GM]	0.8721
Rana et al.[3] [GM & WM]	0.8667
Rana et al.[4]	0.8967

Table 3: Results for Resnet with Learning Rate of 0.0001

Data Type	Pre Trained	Accuracy	MCC	Precision	Recall	F1 Score
Gray Matter	True	**0.948**	**0.895**	**0.948**	**0.948**	**0.948**
	False	0.522	0.064	0.751	0.522	0.363
White Matter	True	**0.963**	**0.925**	**0.955**	**0.955**	**0.955**
	False	0.526	0.052	0.639	0.524	0.444

Table 4: Results for VGG with Learning Rate of 0.0001

Data Type	Pre Trained	Accuracy	MCC	Precision	Recall	F1 Score
Gray Matter	True	**0.925**	**0.848**	**0.926**	**0.925**	**0.926**
	False	0.545	0.139	0.584	0.545	0.535
White Matter	True	**0.940**	**0.880**	**0.933**	**0.933**	**0.933**
	False	0.541	0.098	0.569	0.543	0.498

Table 5: Results for DenseNet with Learning Rate of 0.0001

Data Type	Pre Trained	Accuracy	MCC	Precision	Recall	F1 Score
Gray Matter	True	**0.918**	**0.838**	**0.921**	**0.918**	**0.918**
	False	0.854	0.716	0.862	0.854	0.855
White Matter	True	**0.955**	**0.909**	**0.938**	**0.937**	**0.937**
	False	0.877	0.756	0.871	0.866	0.866

Table 6: Results for MobileNet with Learning Rate of 0.0001

Data Type	Pre Trained	Accuracy	MCC	Precision	Recall	F1 Score
Gray Matter	True	**0.925**	**0.852**	**0.927**	**0.925**	**0.925**
	False	0.534	0.041	0.526	0.534	0.496
White Matter	True	**0.925**	**0.849**	**0.926**	**0.925**	**0.925**
	False	0.604	0.203	0.565	0.569	0.550

Table 7: Results for ShuffleNet with Learning Rate of 0.0001

Data Type	Pre Trained	Accuracy	MCC	Precision	Recall	F1 Score
Gray Matter	True	**0.918**	**0.836**	**0.920**	**0.918**	**0.918**
	False	0.534	0.042	0.533	0.534	0.453
White Matter	True	**0.937**	**0.874**	**0.929**	**0.927**	**0.927**
	False	0.494	0.111	0.531	0.485	0.420

Table 8: Results for SqueezeNet with Learning Rate of 0.0001

Data Type	Pre Trained	Accuracy	MCC	Precision	Recall	F1 Score
Gray Matter	True	**0.873**	**0.747**	**0.874**	**0.873**	**0.873**
	False	0.757	0.542	0.790	0.757	0.748
White Matter	True	**0.948**	**0.898**	**0.912**	**0.910**	**0.910**
	False	0.765	0.530	0.779	0.761	0.755

Table 9: Results for Ensemble Architecture 2 with Pre trained constituent models for Gray Matter and White Matter

Model Block	LR	Accuracy	MCC	Precision	Recall	F1 Score
TriNet1	0.0001	0.903	0.811	0.926	0.923	0.923
QuadNet	0.0001	**0.963**	**0.927**	**0.951**	**0.950**	**0.950**
TriNet2	0.0001	0.955	0.910	0.947	0.947	0.947

Table 10: Results for Ensemble Architecture 1 with Pre trained constituent models for Gray Matter and White Matter

Datatype	LR	Accuracy	MCC	Precision	Recall	F1 Score
WM	0.0001	**0.963**	**0.928**	**0.944**	**0.943**	**0.943**
GM	0.0001	0.948	0.896	0.936	0.935	0.935

The tables report multiple evaluation metric scores including Accuracy, Precision, Recall, F_1 score and MCC score. All scores are reported in the range of (0, 1), except MCC score, which is in the range of (-1, 1). The scores are reported in $Mean \pm Standard\ Deviation$ format. The best scores for each model using the same modality of data but with different window sizes were reported in bold font. Tables 3, 4, 5, 6, 7 and 8 present the performance of Resnet [16], VGG [19], Densenet [18], MobileNet [20], ShuffleNet [21] and SqueezeNet [17], but we modified the input and output layers to handle GM and WM scans. The learning rate was 0.0001. Comparing the overall performance, we can conclude that WM achieved the best performance across all metrics for PD detection. GM also has high performance across all metrics, although the scores were lower than that of WM. Modified Resnet with WM achieved one of the best scores across all metrics among all of the tested models. Using smoothed scans did not improve the performance than using the original scans, probably due to losing fine details. But we notice that no matter testing with the original or smoothed scans, models pretrained with Imagenet data showed significantly better performances than models only trained with MRI data. Table 9 presents different results for Ensemble Architecture 2 using three different model block designs with a learning rate of 0.0001. We only included results using original WM and GM scans, as using smoothed scans gave inferior performance. We can see that QuadNet achieved the highest metric scores. Table 10 shows the results of Ensemble Architecture 1. This architecture was different in the sense that it was only trained for one data modality at a time. Two instances of the model were trained, with one for GM and one for WM. The learning rate was 0.0001. By using the same parameter setting, WM produced the superior scores. Based on our findings, we can say that our methods performed better than related work (Table 2) for analyzing WM and GM. WM provided better information for detecting PD, with the understanding that the smoothed scans might have lost details compared with the orignal scans. It is obvious that our proposed ensemble architectures generated better results than the individual models. Also, architectures pre-trained with the ImageNet database performed better than only trained with a limited set of MRI scans.

5 Occlusion Analysis to Locate Relevant Regions

To understand which regions of the brain are important for the models' decision making process, we performed a slightly modified version of occlusion analysis proposed by Rieke et al. [9]. In this analysis, usually a part of the scan is occluded with a gray or white patch. The occluded region is considered to be important if the probability of detecting the target class decreases compared to the original image. The heatmap of relevance is calculated by sliding the patch across the image and plotting the difference in the probability in red. The brightness of the red-shaded region indicates the importance of the region. In our experiment, the relevance was calculated such that the sum of relevance of all areas was 1. Our heatmaps contain slices taken from the original MRI scan at specific x, y and

z coordinates and the difference in probability at that point. Occlusion analysis was performed on multiple models, but due to page limit, the results of two models that produced the best performance are presented in this section. The models were modified Resnet [16] and Ensemble Architecture 1 [3.4]. All models were pre-trained with the ImageNet [7] dataset, and they were trained with a learning rate of 0.0001. We found that analyzing the GM and WM regions separately produced better results than analyzing the whole brain scan Tahjid et al [22]. Therefore, only models trained on GM or WM were selected for occlusion analysis. The relevance area was calculated from the generated occlusion heatmaps using methods provided by Rieke et al [9].

5.1 Occlusion Analysis for Modified ResNet

Modified Resnet [16] produced the best results out of the 6 individual models as shown in Table 3. Two versions of the model were trained, with one on WM and the other on GM. Figure 4a shows that the Middle Temporal Gyrus and Superior Temporal Gyrus were significant in the decision making process when using WM, followed by the Postcentral Gyrus region. Figure 4b shows that when using GM, the relevance were more evenly distributed, but Middle Temporal Gyrus was once again vital in the decision making process, followed by Middle Frontal Gyrus, Frontal Superior Medial Gyrus, and Thalamus and Superior Temporal Gyrus.

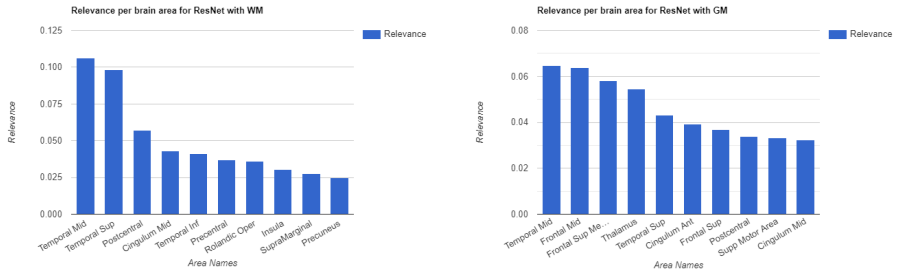

(a) Relevance per brain area for White Matter analysis based on Pretrained ResNet [16]

(b) Relevance per brain area for Gray Matter analysis based on Pretrained ResNet [16]

Fig. 4: Relevance per brain area for PD detection based on Pretrained ResNet

5.2 Occlusion Analysis for Ensemble Architecture - Model 1

Ensemble Architecture 1 [3.4] performed very well when trained on GM and WM as presented in Table 10. The relevance area was computed on 2 versions of the model: WM and GM separately. Figure 5a illustrates the relevance area while

using only WM, showing the Middle Frontal, Middle Occipital and Middle Temporal Gyrus to be the three most relevant areas for decision making. However, the Thalamus, Superior Temporal and Middle Temporal Gyrus appear to be the most relevant when using GM as shown in Figure 5b. Since analyzing WM delivers better detection performance, we believe that, based on our occlusion analysis, the Middle Temporal Gyrus and Middle Frontal should be focused on in future work.

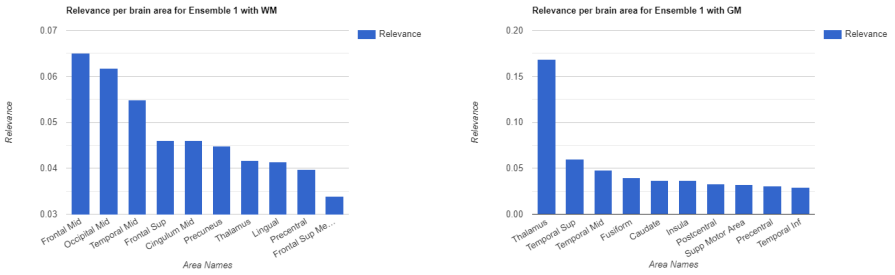

(a) Relevance per brain area for White Matter using Ensemble Architecture 1 with pretrained constituent models

(b) Relevance per brain area for Gray Matter using Ensemble Architecture 1 with pretrained constituent models

Fig. 5: Relevance area based on Ensemble Architecture 1.

6 Conclusion and Future Works

We introduce 2 ensemble architecture structures and demonstrate that their performances outperform individual models for PD detection. By enhancing the concept of ensemble architectures [22], we also explored the performance of detecting PD symptoms in MR images by pre-training with a sufficiently larger number of non-PD related images before training the models with a limited set of PD related WM and GM scans. The learnt image prior significantly enhanced the performance compared to models only trained with the limited MRI scans. In addition, we propose new model block designs with new data modalities for PD Detection. Our results outperform related works in terms of accuracy using similar dataset. This finding suggests that training data unrelated to PD can be used to supplement insufficient PD training data. We also performed occlusion analysis to identify brain regions of high relevance in the decision making process for PD detection.

In future work, we plan to further analyze and understand the decision making process of a model, and focus on the relevant brain regions discovered using occlusion analysis in this paper. We were not able to consult experts and validate our findings regarding relevant areas from occlusion analysis in light of

medical literature due to ongoing Covid-19 situation, however that is also in our future plans. Furthermore, we want to understand which features are better explained by which specific model, based on which we can structure a more efficient ensemble architecture.

Acknowledgment

Data used in the preparation of this article was obtained from the Parkinson's Progression Markers Initiative (PPMI) database (www.ppmi-info.org/data). For up-to-date information on the study, visit www.ppmi-info.org. PPMI is a public-private partnership funded by the Michael J. Fox Foundation for Parkinson's Research and other funding partners listed at www.ppmi-info.org/fundingpartners. Financial support from the Natural Sciences and Engineering Research Council of Canada (NSERC) is gratefully acknowledged.

References

1. N. K. Focke, G. Helms, S. Scheewe, P. M. Pantel, C. G. Bachmann, P. Dechent, J. Ebentheuer, A. Mohr, W. Paulus, C. Trenkwalder, Individual voxel-based subtype prediction can differentiate progressive supranuclear palsy from idiopathic parkinson syndrome and healthy controls, Human Brain Mapping 32 (11) (2011) 1905-1915.
2. G. S. Babu, S. Suresh, B. S. Mahanand, A novel PBL-McRBFN-RFE approach for identification of critical brain regions responsible for parkinson's 235 disease, Expert Systems with Applications 41 (2) (2014) 478-488.
3. B. Rana, A. Juneja, M. Saxena, S. Gudwani, S. S. Kumaran, M. Behari, R. K. Agrawal, Graph-theory-based spectral feature selection for computer aided diagnosis of parkinson's disease using t1-weighted MRI, International Journal of Imaging Systems and Technology 25 (3) (2015) 245-255.
4. B. Rana, A. Juneja, M. Saxena, S. Gudwani, S. S. Kumaran, M. Behari, R. Agrawal, Relevant 3d local binary pattern based features from fused feature descriptor for differential diagnosis of parkinsons disease using structural mri, Biomedical Signal Processing and Control 34 (2017) 134-143.
5. Parkinsons Progression Markers Initiative (PPMI), https://www. 260 ppmi-info.org/, online; accessed 30 September 2019.
6. IXI Dataset, https://brain-development.org/ixi-dataset/, online; accessed 30 September 2019.
7. J. Deng, W. Dong, R. Socher, L.-J. Li, K. Li and L. Fei-Fei, ImageNet: A Large-Scale Hierarchical Image Database,CVPR09. 2009.
8. Olga Russakovsky*, Jia Deng*, Hao Su, Jonathan Krause, Sanjeev Satheesh, Sean Ma, Zhiheng Huang, Andrej Karpathy, Aditya Khosla, Michael Bernstein, Alexander C. Berg and Li Fei-Fei. (* = equal contribution) ImageNet Large Scale Visual Recognition Challenge. IJCV, 2015.
9. J. Rieke,F. Eitel, M. Weygandt,J. Haynes, K. Ritter, Visualizing Convolutional Networks for MRI-based Diagnosis of Alzheimer's Disease, Machine Learning in Clinical Neuroimaging (MLCN), 2018
10. Paszke, A., Gross, S., Massa, F., Lerer, A., Bradbury, J., Chanan, G., Killeen, T.,Lin, Z., Gimelshein, N., Antiga, L., Desmaison, A., Kopf, A., Yang, E., DeVito,

Z.,Raison, M., Tejani, A., Chilamkurthy, S., Steiner, B., Fang, L., Bai, J., Chintala, S.:Pytorch: An imperative style, high-performance deep learning library. In Wallach,H., Larochelle, H., Beygelzimer, A., dAlch e-Buc, F., Fox, E., Garnett, R., eds.:Advances in Neural Information Processing Systems 32. Curran Associates, Inc.(2019) 8024–8035
11. Marcel, S., Rodriguez, Y.: Torchvision the machine-vision package of torch. In:Proceedings of the 18th ACM International Conference on Multimedia. MM '10,New York, NY, USA, Association for Computing Machinery (2010) 1485–1488
12. Kornblith, Simon, Shlens, Jonathon, Le, Quoc. (2018). Do Better ImageNet Models Transfer Better?.
13. Mostafa, T.A., Cheng, I.: Parkinson's Disease Detection Using Ensemble Architecture From MR Images (2020)
14. George A. Miller (1995). WordNet: A Lexical Database for English. Communications of the ACM Vol. 38, No. 11: 39-41.
15. Christiane Fellbaum (1998, ed.) WordNet: An Electronic Lexical Database. Cambridge, MA: MIT Press.
16. He, K., Zhang, X., Ren, S., Sun, J.: Deep residual learning for image recognition.arXiv preprint arXiv:1512.03385 (2015)
17. Iandola, F.N., Moskewicz, M.W., Ashraf, K., Han, S., Dally, W.J., Keutzer, K.:Squeezenet: Alexnet-level accuracy with 50x fewer parameters and¡1mb modelsize. arXiv:1602.07360 (2016)
18. Huang, G., Liu, Z., van der Maaten, L., Weinberger, K.Q.: Densely connectedconvolutional networks (2016)
19. Simonyan, K., Zisserman, A.: Very deep convolutional networks for large-scaleimage recognition (2014)
20. Sandler, M., Howard, A., Zhu, M., Zhmoginov, A., Chen, L.C.: Mobilenetv2: Inverted residuals and linear bottlenecks (2018)
21. Ma, N., Zhang, X., Zheng, H.T., Sun, J.: Shufflenet v2: Practical guidelines forefficient cnn architecture design (2018)
22. Mostafa, T.A., Cheng, I.: Parkinson's Disease Detection Using Ensemble Architecture From MR Images (2020)
23. Mhyre T.R., Boyd J.T., Hamill R.W., Maguire-Zeiss K. (2012) Parkinson's Disease. In: Harris J. (eds) Protein Aggregation and Fibrillogenesis in Cerebral and Systemic Amyloid Disease. Subcellular Biochemistry, vol 65. Springer, Dordrecht
24. B. Peng, S. Wang, Z. Zhou, Y. Liu, B. Tong, T. Zhang, and Y. Dai, "A multilevel-roi-features-based machine learning method for detection of morphometric biomarkers in parkinson's disease," Neuroscience letters, vol. 651, pp. 88–94, 2017
25. H.-C. Cheng, C. M. Ulane, and R. E. Burke, Clinical progression in Parkinson disease and the neurobiology of axons, Annals of Neurology, vol. 67, no. 6, pp. 715725, Jun. 2010.
26. D. Athauda et al., Exenatide once weekly versus placebo in Parkinsons disease: a randomised, double-blind, placebo-controlled trial, The Lancet, vol. 390, no. 10103, pp. 16641675, Oct. 2017.
27. S. Pazhanirajan and P. Dhanalakshmi, "Classification of parkinson's disease using mri images," International Journal of Computer Science and Software Engineering, vol. 5, no. 10, p. 233, 2016
28. West C., Soltaninejad S., Cheng I. (2020) Assessing the Capability of Deep-Learning Models in Parkinson's Disease Diagnosis. In: McDaniel T., Berretti S., Curcio I., Basu A. (eds) Smart Multimedia. ICSM 2019. Lecture Notes in Computer Science, vol 12015. Springer, Cham